

---

# Learning Factorized Multimodal Representations

---

Yao-Hung Hubert Tsai <sup>\*1</sup> Paul Pu Liang <sup>\*1</sup>  
 Amir Zadeh <sup>2</sup> Louis-Philippe Morency <sup>2</sup> Ruslan Salakhutdinov <sup>1</sup>  
 Machine Learning Department<sup>1</sup> Language Technologies Institute<sup>2</sup>, Carnegie Mellon University

## Abstract

Learning representations of multimodal data is a fundamentally complex research problem due to the presence of multiple sources of information. To address the complexities of multimodal data, we argue that suitable representation learning models should: 1) factorize representations according to independent factors of variation in the data, capture important features for both 2) discriminative and 3) generative tasks, and 4) couple both modality-specific and multimodal information. To encapsulate all these properties, we propose the Multimodal Factorization Model (MFM) that factorizes multimodal representations into two sets of independent factors: *multimodal discriminative* factors and *modality-specific generative* factors. Multimodal discriminative factors are shared across all modalities and contain joint multimodal features required for discriminative tasks such as predicting sentiment. Modality-specific generative factors are unique for each modality and contain the information required for generating data. Our experimental results show that our model is able to learn meaningful multimodal representations and achieve state-of-the-art or competitive performance on five multimodal datasets. Our model also demonstrates flexible generative capabilities by conditioning on the independent factors. We further interpret our factorized representations to understand the interactions that influence multimodal learning.

## 1 Introduction

Multimodal machine learning involves learning from data across multiple modalities. It is a challenging yet crucial research with real-world applications such as robotics [1; 30], dialogue systems [42; 43], intelligent tutoring systems [60; 31; 41], and healthcare diagnosis [38; 13]. At the heart of many multimodal modeling tasks lies the challenge of learning suitable representations from multiple modalities. For example, analyzing videos and other multimedia content requires learning multimodal representations across the language, visual, and acoustic modalities [33]. We argue that multimodal representations should possess the following properties: 1) *Factorized*: Different explanatory factors of the data tend to change independently of each other [4]. Suitable multimodal representations should factorize according to these independent factors of variation. 2) *Discriminative*: Multimodal representations should encapsulate the important features that are required for discriminative tasks. 3) *Generative*: Inspired by the recent success of generative approaches [24; 57], suitable multimodal representations should also capture the features required for multimodal data generation. 4) *Specificity*: Multimodal representations should encompass both modality-specific and multimodal factors. Modality-specific factors represent features unique to each modality while multimodal factors represent joint features shared across all modalities [2].

Given input data  $\mathbf{X}_1, \dots, \mathbf{X}_M$  from  $M$  modalities and labels  $\mathbf{Y}$ , previous research has focused on learning discriminative multimodal representations (property 2) by modeling  $P(\mathbf{Y}|\mathbf{X}_1, \dots, \mathbf{X}_M)$  [66; 67; 65; 7; 59; 58]. Some previous work learn generative multimodal representations (property 3) by modeling the joint distribution of multimodal data  $P(\mathbf{X}_1, \dots, \mathbf{X}_M)$  and using these representations

---

<sup>\*</sup>equal contributions

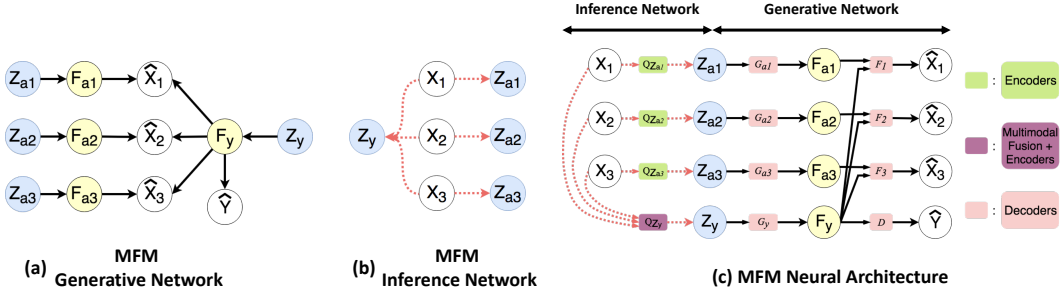


Figure 1: Illustration of the proposed Multimodal Factorization Model (MFM) with three modalities. MFM factorizes multimodal representations into *multimodal discriminative factors*  $\mathbf{F}_y$  and *modality-specific generative factors*  $\mathbf{F}_{a\{1:M\}}$ . (a) MFM Generative Network with latent variables  $\{\mathbf{Z}_y, \mathbf{Z}_{a\{1:M\}}\}$ , factors  $\{\mathbf{F}_y, \mathbf{F}_{a\{1:M\}}\}$ , generated multimodal data  $\hat{\mathbf{X}}_{1:3}$  and labels  $\hat{\mathbf{Y}}$ . (b) MFM Inference Network. (c) MFM Neural Architecture. Best viewed zoomed in and in color.

for discriminative tasks [55; 52; 56]. However, there has been a lack of research on multimodal representation learning that simultaneously satisfies all aforementioned properties, especially on learning factorized and specific representations. In fact, we hypothesize that the factorized property is the most important because: 1) factorized representations further assist in discriminative tasks due to improved distillation of discriminative features in a structured manner, 2) factorized representations improve generative capabilities through flexible generation based on the factorized variables, and 3) factorized representations have the potential to be more interpretable than their unfactored counterparts.

To encapsulate all these properties, we propose the Multimodal Factorization Model (MFM) for multimodal representation learning. MFM (Figure 1) factorizes the multimodal representation into two sets of independent factors: *multimodal discriminative factors* and *modality-specific generative factors*. The multimodal discriminative factor, denoted as  $\mathbf{F}_y$ , is shared across all modalities and contains joint multimodal features required for discriminative tasks. Modality-specific generative factors, denoted as  $\mathbf{F}_{a\{1:M\}}$ , are unique for each modality and contain information required for generating each modality. MFM learns factorized representations using a hybrid generative-discriminative objective which models the joint distribution over multimodal data. This enables MFM to learn multimodal representations that are simultaneously *factorized*, *discriminative*, *generative* and *specific*.

We design an extensive set of experiments to show that MFM learns improved multimodal representations with the following characteristics: 1) The multimodal discriminative factors achieve state-of-the-art or competitive performance on five multimodal datasets. 2) The independent factors allow flexible generation of data with respect to multimodal discriminative factors (labels) and modality-specific generative factors (styles). 3) We interpret both overall and fine-grained trends of our factorized representations using dependency-based and gradient-based methods. This allows us to understand the contributions of individual factors during multimodal prediction and generation.

## 2 Multimodal Factorization Model

Multimodal Factorization Model (MFM) is a latent variable model (Figure 1 (a)) with conditional independence assumptions over multimodal discriminative factors and modality-specific generative factors. According to these assumptions, we propose a factorization over the joint distribution of multimodal data (Section 2.1). Since exact posterior inference on this factorized distribution can be intractable (as explained later in this section), we propose an approximate inference algorithm based on minimizing a joint-distribution Wasserstein distance over multimodal data (Section 2.2). Finally, we derive the MFM objective by approximating the joint-distribution Wasserstein distance via a generalized mean-field assumption.

**Notation:** We define  $\mathbf{X}_{1:M}$  as the multimodal data from  $M$  modalities and  $\mathbf{Y}$  as the labels, with joint distribution  $P_{\mathbf{X}_{1:M}, \mathbf{Y}} = P(\mathbf{X}_{1:M}, \mathbf{Y})$ . Let  $\hat{\mathbf{X}}_{1:M}$  denote the generated multimodal data and  $\hat{\mathbf{Y}}$  denote the generated labels, with joint distribution  $P_{\hat{\mathbf{X}}_{1:M}, \hat{\mathbf{Y}}} = P(\hat{\mathbf{X}}_{1:M}, \hat{\mathbf{Y}})$ .

### 2.1 Factorized Multimodal Representations

To factorize multimodal representations into multimodal discriminative factors and modality-specific generative factors, MFM assumes a Bayesian network structure as shown in Figure 1 (a). In this

graphical model, factors  $\mathbf{F}_y$  and  $\mathbf{F}_{\mathbf{a}\{1:M\}}$  are generated from mutually independent latent variables  $\mathbf{Z} = [\mathbf{Z}_y, \mathbf{Z}_{\mathbf{a}\{1:M\}}]$  with prior  $P_{\mathbf{Z}}$ . In particular,  $\mathbf{Z}_y$  generates the multimodal discriminative factor  $\mathbf{F}_y$  and  $\mathbf{Z}_{\mathbf{a}\{1:M\}}$  generate modality-specific generative factors  $\mathbf{F}_{\mathbf{a}\{1:M\}}$ . By construction,  $\mathbf{F}_y$  contributes to the generation of  $\hat{\mathbf{Y}}$  while  $\{\mathbf{F}_y, \mathbf{F}_{\mathbf{a}_i}\}$  both contribute to the generation of  $\hat{\mathbf{X}}_i$ . As a result, the joint distribution  $P(\hat{\mathbf{X}}_{1:M}, \hat{\mathbf{Y}})$  can be factorized as follows:

$$\begin{aligned} P(\hat{\mathbf{X}}_{1:M}, \hat{\mathbf{Y}}) &= \int_{\mathbf{F}, \mathbf{Z}} P(\hat{\mathbf{X}}_{1:M}, \hat{\mathbf{Y}}|\mathbf{F})P(\mathbf{F}|\mathbf{Z})P(\mathbf{Z})d\mathbf{F}d\mathbf{Z} \\ &= \int_{\substack{\mathbf{F}_y, \mathbf{F}_{\mathbf{a}\{1:M\}} \\ \mathbf{Z}_y, \mathbf{Z}_{\mathbf{a}\{1:M\}}} } \left( P(\hat{\mathbf{Y}}|\mathbf{F}_y) \prod_{i=1}^M P(\hat{\mathbf{X}}_i|\mathbf{F}_{\mathbf{a}_i}, \mathbf{F}_y) \right) \left( P(\mathbf{F}_y|\mathbf{Z}_y) \prod_{i=1}^M P(\mathbf{F}_{\mathbf{a}_i}|\mathbf{Z}_{\mathbf{a}_i}) \right) \left( P(\mathbf{Z}_y) \prod_{i=1}^M P(\mathbf{Z}_{\mathbf{a}_i}) \right) d\mathbf{F}d\mathbf{Z}, \end{aligned} \quad (1)$$

with  $d\mathbf{F} = d\mathbf{F}_y \prod_{i=1}^M d\mathbf{F}_{\mathbf{a}_i}$  and  $d\mathbf{Z} = d\mathbf{Z}_y \prod_{i=1}^M d\mathbf{Z}_{\mathbf{a}_i}$ .

Exact posterior inference in Equation (1) may be analytically intractable due to the integration over  $\mathbf{Z}$ . We therefore resort to using an approximate inference distribution  $Q(\mathbf{Z}|\mathbf{X}_{1:M}, \mathbf{Y})$ , detailed in the following subsection. As a result, MFM can be viewed as an autoencoding structure that consists of encoder (inference) and decoder (generative) modules (Figure 1 (c)). The encoder module for  $Q(\cdot|\cdot)$  allows us to easily sample  $\mathbf{Z}$  from an approximate posterior. The decoder modules are parametrized according to the factorization of  $P(\hat{\mathbf{X}}_{1:M}, \hat{\mathbf{Y}}|\mathbf{Z})$  as given by Equation (1) and Figure 1 (a).

## 2.2 Minimizing Joint-Distribution Wasserstein Distance over Multimodal Data

Two common choices for approximate inference in autoencoding structures are Variational Autoencoders (VAEs) [24] and Wasserstein Autoencoders (WAEs) [57]. The former optimizes the evidence lower bound objective (ELBO), and the latter derives an approximation for the primal form of the Wasserstein distance. We consider the latter since it simultaneously results in better latent factor disentanglement [49] and better sample generation quality than its counterparts [9; 19; 24]. However, WAEs are designed for unimodal data and do not consider factorized distributions over latent variables that generate multimodal data. Therefore, we propose an extension of WAEs to handle factorized joint distributions over multimodal data.

As suggested by [24], we adopt the design of nonlinear mappings (i.e. neural network architectures) in an encoder and decoder (Figure 1 (c)). As the choice of an encoder for  $Q(\mathbf{Z}|\mathbf{X}_{1:M}, \mathbf{Y})$ , we learn a deterministic mapping  $Q_{enc} : \mathbf{X}_{1:M}, \mathbf{Y} \rightarrow \mathbf{Z}$  [49; 57]. For the decoder, we define the generation process from latent variables as  $G_y : \mathbf{Z}_y \rightarrow \mathbf{F}_y$ ,  $G_{\mathbf{a}\{1:M\}} : \mathbf{Z}_{\mathbf{a}\{1:M\}} \rightarrow \mathbf{F}_{\mathbf{a}\{1:M\}}$ ,  $D : \mathbf{F}_y \rightarrow \hat{\mathbf{Y}}$ , and  $F_{1:M} : \mathbf{F}_y, \mathbf{F}_{\mathbf{a}\{1:M\}} \rightarrow \hat{\mathbf{X}}_{1:M}$ , where  $G_y, G_{\mathbf{a}\{1:M\}}, D$  and  $F_{1:M}$  are deterministic functions parametrized by neural networks.

Let  $W_c(P_{\mathbf{X}_{1:M}, \mathbf{Y}}, P_{\hat{\mathbf{X}}_{1:M}, \hat{\mathbf{Y}}})$  denote the joint-distribution Wasserstein distance over multimodal data under cost function  $c_{X_i}$  and  $c_Y$ . We choose the squared cost  $c(a, b) = \|a - b\|_2^2$ , allowing us to minimize the 2-Wasserstein distance. The cost function can be defined not only on static data but also on time series data such as text, audio and videos. For example, given time series data  $\mathbf{X} = [X^1, X^2, \dots, X^T]$  and  $\hat{\mathbf{X}} = [\hat{X}^1, \hat{X}^2, \dots, \hat{X}^T]$ , we define  $c(\mathbf{X}, \hat{\mathbf{X}}) = \sum_{t=1}^T \|X^t - \hat{X}^t\|_2^2$ .

Using the conditional independence assumptions in Equation (1),  $W_c(P_{\mathbf{X}_{1:M}, \mathbf{Y}}, P_{\hat{\mathbf{X}}_{1:M}, \hat{\mathbf{Y}}})$  can be expressed as:

**Proposition 1.** *For any functions  $G_y : \mathbf{Z}_y \rightarrow \mathbf{F}_y$ ,  $G_{\mathbf{a}\{1:M\}} : \mathbf{Z}_{\mathbf{a}\{1:M\}} \rightarrow \mathbf{F}_{\mathbf{a}\{1:M\}}$ ,  $D : \mathbf{F}_y \rightarrow \hat{\mathbf{Y}}$ , and  $F_{1:M} : \mathbf{F}_{\mathbf{a}\{1:M\}}, \mathbf{F}_y \rightarrow \hat{\mathbf{X}}_{1:M}$ , we have  $W_c(P_{\mathbf{X}_{1:M}, \mathbf{Y}}, P_{\hat{\mathbf{X}}_{1:M}, \hat{\mathbf{Y}}}) =$*

$$\inf_{Q_{\mathbf{Z}}=P_{\mathbf{Z}}} \mathbf{E}_{P_{\mathbf{X}_{1:M}, \mathbf{Y}}} \mathbf{E}_{Q_{\mathbf{Z}}|\mathbf{X}_{1:M}, \mathbf{Y}}} \left[ \sum_{i=1}^M c_{X_i}(\mathbf{X}_i, F_i(G_{\mathbf{a}_i}(\mathbf{Z}_{\mathbf{a}_i}), G_y(\mathbf{Z}_y))) + c_Y(\mathbf{Y}, D(G_y(\mathbf{Z}_y))) \right], \quad (2)$$

where  $P_{\mathbf{Z}}$  is the prior over  $\mathbf{Z} = [\mathbf{Z}_y, \mathbf{Z}_{\mathbf{a}\{1:M\}}]$  and  $Q_{\mathbf{Z}}$  is the aggregated posterior of the proposed approximate inference distribution  $Q(\mathbf{Z}|\mathbf{X}_{1:M}, \mathbf{Y})$ .

*Proof:* The proof is adapted from Tolstikhin *et al.* [57]. The two differences are: (1) we show that  $P(\hat{\mathbf{X}}_{1:M}, \hat{\mathbf{Y}}|\mathbf{Z} = z)$  are Dirac for all  $z \in \mathcal{Z}$ , and (2) we use the fact that  $c((\mathbf{X}_{1:M}, \mathbf{Y}), (\hat{\mathbf{X}}_{1:M}, \hat{\mathbf{Y}})) = \sum_{i=1}^M c_{X_i}(\mathbf{X}_i, \hat{\mathbf{X}}_i) + c_Y(\mathbf{Y}, \hat{\mathbf{Y}})$ . Please refer to the supplementary material for proof details. ■

The constraint on  $Q_{\mathbf{Z}} = P_{\mathbf{Z}}$  in Proposition (1) is hard to satisfy. To obtain a numerical solution, we first relax the constraint by performing a generalized mean field assumption on  $Q$  according to the conditional independence as shown in the inference network of Figure 1 (b):

$$Q(\mathbf{Z}|\mathbf{X}_{1:M}, \mathbf{Y}) := Q(\mathbf{Z}|\mathbf{X}_{1:M}) := Q(\mathbf{Z}_{\mathbf{y}}|\mathbf{X}_{1:M}) \prod_{i=1}^M Q(\mathbf{Z}_{\mathbf{a}_i}|\mathbf{X}_i). \quad (3)$$

The intuition here is based on our design that  $\mathbf{Z}_{\mathbf{y}}$  generates the multimodal discriminative factor  $\mathbf{F}_{\mathbf{y}}$  and  $\mathbf{Z}_{\mathbf{a}\{1:M\}}$  generate modality-specific generative factors  $\mathbf{F}_{\mathbf{a}\{1:M\}}$ . Therefore, the inference for  $\mathbf{Z}_{\mathbf{y}}$  should depend on all modalities  $\mathbf{X}_{1:M}$  and the inference for  $\mathbf{Z}_{\mathbf{a}_i}$  should depend only on the specific modality  $\mathbf{X}_i$ . Then, we let  $\mathcal{Q}$  be a nonparametric set of all encoders that fulfill the factorization in Equation (3). A penalty term is added into our objective to find the  $Q(\mathbf{Z}|\cdot) \in \mathcal{Q}$  that is the closest to prior  $P_{\mathbf{Z}}$ , thereby approximately enforcing the constraint  $Q_{\mathbf{Z}} = P_{\mathbf{Z}}$ :

$$\min_{F, G_{\mathbf{a}\{1:M\}}, G_{\mathbf{y}}, D} \inf_{Q(\mathbf{Z}|\cdot) \in \mathcal{Q}} \mathbf{E}_{P_{\mathbf{X}_{1:M}}, \mathbf{Y}} \mathbf{E}_{Q(\mathbf{Z}_{\mathbf{a}_1}|\mathbf{X}_1)} \cdots \mathbf{E}_{Q(\mathbf{Z}_{\mathbf{a}_M}|\mathbf{X}_M)} \mathbf{E}_{Q(\mathbf{Z}_{\mathbf{y}}|\mathbf{X}_{1:M})} \left[ \sum_{i=1}^M c_{X_i} \left( \mathbf{X}_i, F(G_{\mathbf{a}_i}(\mathbf{Z}_{\mathbf{a}_i}), G_{\mathbf{y}}(\mathbf{Z}_{\mathbf{y}})) \right) + c_{\mathbf{Y}} \left( \mathbf{Y}, D(G_{\mathbf{y}}(\mathbf{Z}_{\mathbf{y}})) \right) \right] + \lambda \mathcal{MMD}(Q_{\mathbf{Z}}, P_{\mathbf{Z}}), \quad (4)$$

where  $\lambda$  is a hyper-parameter and  $\mathcal{MMD}$  is the Maximum Mean Discrepancy [16] as a divergence measure between  $Q_{\mathbf{Z}}$  and  $P_{\mathbf{Z}}$ . The prior  $P_{\mathbf{Z}}$  is chosen as a centered isotropic Gaussian  $\mathcal{N}(\mathbf{0}, \mathbf{I})$ , so that it implicitly enforces independence between the latent variables  $\mathbf{Z} = [\mathbf{Z}_{\mathbf{y}}, \mathbf{Z}_{\mathbf{a}\{1,M\}}]$  [19; 24; 49].

Equation (4) represents our hybrid generative-discriminative optimization objective over multimodal data: the first loss term  $\sum_{i=1}^M c_{X_i}(\mathbf{X}_i, F(G_{\mathbf{a}_i}(\mathbf{Z}_{\mathbf{a}_i}), G_{\mathbf{y}}(\mathbf{Z}_{\mathbf{y}})))$  is the generative objective based on reconstruction of multimodal data and the second term  $c_{\mathbf{Y}}(\mathbf{Y}, D(G_{\mathbf{y}}(\mathbf{Z}_{\mathbf{y}})))$  is the discriminative objective. In practice we compute the expectations in Equation (4) using empirical estimates over the training data. The neural architecture of MFM is illustrated in Figure 1 (c).

### 3 Experiments

In this section, we evaluate MFM by designing three sets of experiments: First, we demonstrate improved discriminative performance and flexible generation on a simple multimodal synthetic digit dataset. Next, we evaluate the advantages of factorized multimodal representations on complex multimodal time series datasets. The inferred discriminative features in MFM demonstrate state-of-the-art or competitive performance on these multimodal prediction tasks. Finally, we interpret both overall and fine-grained trends of our factorized representations using dependency-based and gradient-based methods.

#### 3.1 Encoder and Decoder Design

We now discuss the implementation choices for the MFM neural architecture in Figure 1 (c). The encoder  $Q(\mathbf{Z}_{\mathbf{y}}|\mathbf{X}_{1:M})$  can be parametrized by any model that performs multimodal fusion [37; 66; 67]. For multimodal synthetic image datasets, we adopt Convolutional Neural Networks (CNNs) and Fully-Connected Neural Networks (FCNNs) with late fusion [37; 3] as our encoder  $Q(\mathbf{Z}_{\mathbf{y}}|\mathbf{X}_{1:M})$ . The remaining functions in MFM are also parametrized by CNNs and FCNNs. For multimodal time series datasets, we choose the Memory Fusion Network (MFN) [66] as our encoder  $Q(\mathbf{Z}_{\mathbf{y}}|\mathbf{X}_{1:M})$ . We use Long Short-term Memory (LSTM) [20] networks for functions  $Q(\mathbf{Z}_{\mathbf{a}\{1:M\}}|\mathbf{X}_{1:M})$ , decoder LSTM networks [11] for functions  $F_{1:M}$ , and FCNNs for functions  $G_{\mathbf{y}}, G_{\mathbf{a}\{1:M\}}$  and  $D$ . Details are provided in the supplementary material and the code is publicly available at <anonymous>.

#### 3.2 Multimodal Synthetic Image Dataset

In this section, we study MFM on a synthetic image dataset that considers SVHN [35] and MNIST [28] as the two modalities. SVHN and MNIST are digit images with different styles but the same labels (digits 0 ~ 9). We randomly pair 100,000 SVHN and MNIST images that have the same label, synthesizing a multimodal image dataset which we call SVHN-MNIST. 80,000 pairs are used for training and the rest for testing. To justify that MFM is able to learn improved multimodal representations, we show both classification and generation results on SVHN-MNIST in Figure 5.

**Digit Classification:** We perform experiments on both unimodal and multimodal classification tasks. UM denotes a unimodal baseline that performs prediction given only one modality as input. On

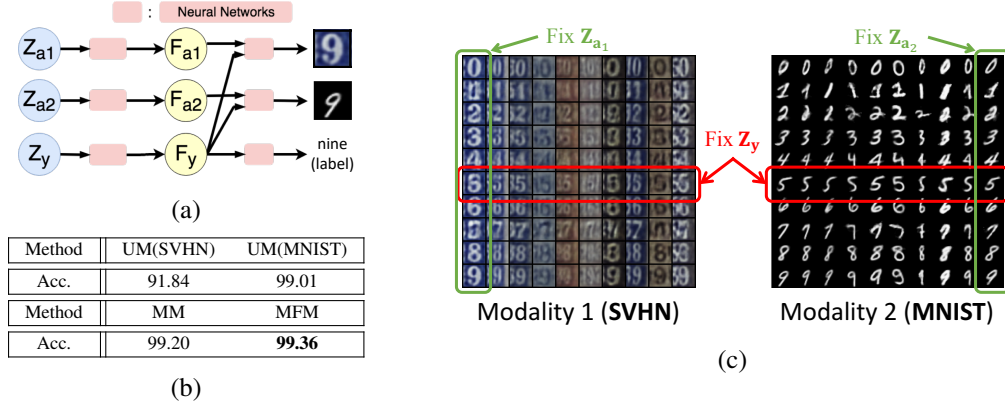


Figure 5: (a) MFM generative network for multimodal static dataset SVHN-MNIST, (b) Unimodal and multimodal classification accuracies. (c) Conditional generation for SVHN and MNIST digits.

the other hand, MM denotes a multimodal discriminative baseline that performs predictions given two images [37]. We compare the results for UM(SVHN), UM(MNIST), MM and MFM on SVHN-MNIST in Figure 5 (b). We achieve better classification performance from unimodal to multimodal which is not surprising since more information is given. More importantly, MFM outperforms MM, which suggests that MFM learns improved factorized representations for discriminative tasks.

**Digit Generation:** We now generate images using the MFM generative network as shown in Figure 5 (a). We fix one variable out of  $Z = [Z_{a1}, Z_{a2}, \text{ and } Z_y]$  and randomly sample the other two variables from prior  $P_Z$ . From Figure 5 (c), we observe that MFM shows flexible generation of SVHN and MNIST images based on labels and styles. This suggests that MFM is indeed able to factorize multimodal representations into multimodal discriminative factors (labels) and modality-specific generative factors (styles).

### 3.3 Multimodal Time Series Datasets

In this section, we transition to more challenging multimodal time series datasets. All the datasets consist of videos where one speaker is in front of the camera. Features are extracted from the language (GloVe word embeddings [40]), visual (Facet [22]), and acoustic (COVAREP [12]) modalities. For a detailed description of feature extraction, please refer to the supplementary material. We experiment with the following five multimodal time series datasets across three domains:

- (1) Multimodal Personality Trait Recognition. **POM** [39] contains 903 movie review videos annotated for the following personality traits: confident (con), passionate (pas), voice pleasant (voi), dominant (dom), credible (cre), vivid (viv), expertise (exp), entertaining (ent), reserved (res), trusting (tru), relaxed (rel), outgoing (out), thorough (tho), nervous (ner), persuasive (per) and humorous (hum). The short form is indicated in parenthesis.
- (2) Multimodal Sentiment Analysis. **CMU-MOSI** [68] is a collection of 2199 monologue opinion video clips each annotated with sentiment. **ICT-MMMO** [62] consists of 340 online social review videos annotated for sentiment. **YouTube** [33] contains 269 product review and opinion video segments from YouTube each annotated for sentiment.
- (3) Multimodal Emotion Recognition. **IEMOCAP** [6] consists of 302 videos of recorded dyadic dialogues. The videos are divided into multiple segments each annotated for the presence of 6 discrete emotions (happy, sad, angry, frustrated, excited and neutral), resulting in a total of 7318 segments in the dataset.

We report results using the following metrics:  $A^C$  = multiclass accuracy across  $C$  classes,  $F1 = F1$  score,  $MAE$  = Mean Absolute Error,  $r$  = Pearson’s correlation.

**Multimodal Prediction:** We first compare the performance of MFM with existing multimodal prediction methods. For a detailed description of the baselines, we point the reader to MFN [66], MARN [67], TFN [65], BC-LSTM [45], MV-LSTM [47], EF-LSTM [21; 15; 50], DF [37], MV-HCRF [53; 54], EF-HCRF [46; 34], C-MKL [44], SAL-CNN [61], THMM [33], SVM-MD [68] and RF [5]. From Table 1, we first observe that the best performing baseline results are achieved by different models across different datasets (most notably MFN, MARN and TFN). On the other hand, MFM consistently achieves state-of-the-art or competitive results for all five multimodal datasets. We believe that by our MFM design, the multimodal discriminative factor  $F_y$  has successfully learned

Table 1: Results for multimodal speaker traits recognition on POM, multimodal sentiment analysis on CMU-MOSI, ICT-MMMO, YouTube, and multimodal emotion recognition on IEMOCAP. SOTA1 and SOTA2 refer to the previous best and second best state-of-the-art respectively. Symbols depict the baseline giving the result: # *MFN*, ‡ *MARN*, \* *TFN*, † *BC-LSTM*, ◊ *MV-LSTM*, § *EF-LSTM*, † *DF*, ♡ *SVM*, • *RF*. For a detailed table with all results, please refer to the supplementary. Best results are in bold and  $\Delta_{SOTA}$  shows the performance improvement over SOTA1. MFM achieves state-of-the-art or competitive performance on all datasets.

Dataset Task Metric	POM Personality Traits															
	Con	Pas	Voi	Dom	Cre	Viv	Exp	Ent	Res	Tru	Rel	Out	Tho	Ner	Per	Hum
SOTA2	0.359 <sup>†</sup>	0.425 <sup>†</sup>	0.131 <sup>◊</sup>	0.234 <sup>†</sup>	0.358 <sup>†</sup>	0.417 <sup>†</sup>	0.450 <sup>†</sup>	0.361 <sup>†</sup>	0.295 <sup>◊</sup>	0.237 <sup>◊</sup>	0.119 <sup>◊</sup>	0.238 <sup>◊</sup>	0.363 <sup>†</sup>	0.258 <sup>◊</sup>	0.344 <sup>†</sup>	0.319 <sup>†</sup>
SOTA1	0.395 <sup>#</sup>	0.428 <sup>#</sup>	0.193 <sup>#</sup>	0.313 <sup>#</sup>	0.367 <sup>#</sup>	0.431 <sup>#</sup>	0.452 <sup>#</sup>	0.395 <sup>#</sup>	0.333 <sup>#</sup>	<b>0.296<sup>#</sup></b>	0.255 <sup>#</sup>	0.259 <sup>#</sup>	0.381 <sup>#</sup>	0.318 <sup>#</sup>	<b>0.377<sup>#</sup></b>	0.386 <sup>#</sup>
MFM	<b>0.431</b>	<b>0.450</b>	<b>0.197</b>	<b>0.411</b>	<b>0.380</b>	<b>0.448</b>	<b>0.467</b>	<b>0.452</b>	<b>0.368</b>	0.212	<b>0.309</b>	<b>0.333</b>	<b>0.404</b>	<b>0.333</b>	0.334	<b>0.408</b>
$\Delta_{SOTA}$	†0.036	†0.022	†0.004	†0.097	†0.013	†0.017	†0.015	†0.057	†0.035	–	†0.054	†0.074	†0.023	†0.015	–	†0.022

Dataset Task Metric	CMU-MOSI Sentiment					ICT-MMMO Sentiment		YouTube Sentiment	
	A <sup>2</sup>	F1	A <sup>7</sup>	MAE	r	A <sup>2</sup>	F1	A <sup>3</sup>	F1
SOTA2	77.1 <sup>‡</sup>	77.0 <sup>‡</sup>	34.1 <sup>#</sup>	0.968 <sup>‡</sup>	0.625 <sup>‡</sup>	72.5 <sup>*</sup>	72.6 <sup>*</sup>	48.3 <sup>‡</sup>	45.0 <sup>#</sup>
SOTA1	<b>77.4<sup>#</sup></b>	<b>77.3<sup>#</sup></b>	34.7 <sup>‡</sup>	0.965 <sup>#</sup>	0.632 <sup>#</sup>	73.8 <sup>#</sup>	73.1 <sup>#</sup>	51.7 <sup>#</sup>	51.6 <sup>#</sup>
MFM	77.3	77.2	<b>35.4</b>	<b>0.961</b>	<b>0.661</b>	<b>76.3</b>	<b>76.2</b>	<b>53.3</b>	<b>52.4</b>
$\Delta_{SOTA}$	–	–	†0.7	↓0.004	†0.029	†2.5	†3.1	†1.6	†0.8

Dataset Task Metric	IEMOCAP Emotions											
	Happy		Sad		Angry		Frustrated		Excited		Neutral	
	A <sup>2</sup>	F1	A <sup>2</sup>	F1	A <sup>2</sup>	F1	A <sup>2</sup>	F1	A <sup>2</sup>	F1	A <sup>2</sup>	F1
SOTA2	86.7 <sup>‡</sup>	84.2 <sup>§</sup>	83.4 <sup>*</sup>	81.7 <sup>†</sup>	85.1 <sup>◊</sup>	84.5 <sup>§</sup>	79.5 <sup>‡</sup>	76.6 <sup>‡</sup>	89.6 <sup>‡</sup>	86.3 <sup>#</sup>	68.8 <sup>§</sup>	67.1 <sup>§</sup>
SOTA1	90.1 <sup>#</sup>	85.3 <sup>#</sup>	85.8 <sup>#</sup>	82.8 <sup>*</sup>	87.0 <sup>#</sup>	86.0 <sup>#</sup>	80.3 <sup>#</sup>	<b>76.8<sup>#</sup></b>	89.8 <sup>#</sup>	<b>87.1<sup>‡</sup></b>	71.8 <sup>#</sup>	<b>68.5<sup>§</sup></b>
MFM	<b>90.2</b>	<b>85.8</b>	<b>88.4</b>	<b>86.1</b>	<b>87.5</b>	<b>86.7</b>	<b>80.4</b>	74.5	<b>90.0</b>	<b>87.1</b>	<b>72.1</b>	68.1
$\Delta_{SOTA}$	†0.1	†0.5	†2.6	†3.3	†0.5	†0.7	†0.1	–	†0.2	–	†0.3	–

more meaningful representations by distilling discriminative features. This highlights the benefit of learning factorized multimodal representations towards discriminative tasks.

**Ablation Study:** In Figure 6, we present the models  $M_{\{A,B,C,D,E\}}$  used for ablation studies. These ablations consider several variants of the design decisions chosen in MFM. We consider the choices of using a multimodal discriminative factor, a hybrid generative-discriminative objective, factorized generative-discriminative factors and modality-specific generative factors. From Table 2, we observe the following general trends: 1) using a multimodal discriminative factor performs better than using modality-specific discriminative factors, 2) adding generative capabilities to the model improves discriminative performance, 3) factorizing representations into generative and discriminative factors improves performance, and 4) using modality-specific generative factors performs better than using a multimodal generative factor. These observations support our design choices of factorizing multimodal representations into multimodal discriminative factors and modality-specific generative factors.

### 3.4 Interpreting Multimodal Representations

In this section, we devise dependency-based and gradient-based methods to study our multimodal representations. The dependency-based method is designed to summarize the overall contributions of each modality towards the multimodal representations. This interpretation method happens at the resolution of entire datasets. The gradient-based method is designed to obtain a more fine-grained analysis of the relationships between each modality and the prediction task. This interpretation method will help to visualize contributions from individual modalities that occur only in particular short segments of a time series. Both methods allow us to analyze how individual factors in MFM influence the dynamics of multimodal prediction and generation.

**Dependency-based Interpretation:** We are interested in summarizing the contribution of each modality towards the multimodal representations. Since the multimodal discriminative factor  $F_y$  is a common cause of  $\hat{X}_{1:M}$ , we can compare  $\text{Depen}(F_y, \hat{X}_1), \dots, \text{Depen}(F_y, \hat{X}_M)$ , where  $\text{Depen}(\cdot, \cdot)$  stands for a dependency measure between  $F_y$  and generated modality  $\hat{X}_i$ . Higher  $\text{Depen}(F_y, \hat{X}_i)$  in-

Table 2: Results for ablation studies on CMU-MOSI. Best results in bold. All the components in MFM are necessary for best performance.

Variants	Multimodal Discriminative Factor	Hybrid Gen.-Discr. Objective	Factorized Gen.-Discr. Factors	Modal.-Speci. Generative Factors	Dataset : CMU-MOSI Task : Sentiment				
					A <sup>2</sup>	F1	A <sup>7</sup>	MAE	r
M <sub>E</sub>	yes	no	–	–	76.1	76.0	28.7	1.043	0.634
M <sub>D</sub>	no	no	–	–	74.6	74.7	28.7	1.024	0.626
M <sub>C</sub>	yes	yes	no	–	76.5	76.5	31.9	1.071	0.647
M <sub>B</sub>	no	yes	no	–	74.9	75.0	33.1	1.023	0.627
M <sub>A</sub>	yes	yes	yes	no	75.1	75.1	32.4	1.039	0.645
<b>MFM</b>	yes	yes	yes	yes	<b>77.3</b>	<b>77.2</b>	<b>35.4</b>	<b>0.961</b>	<b>0.661</b>

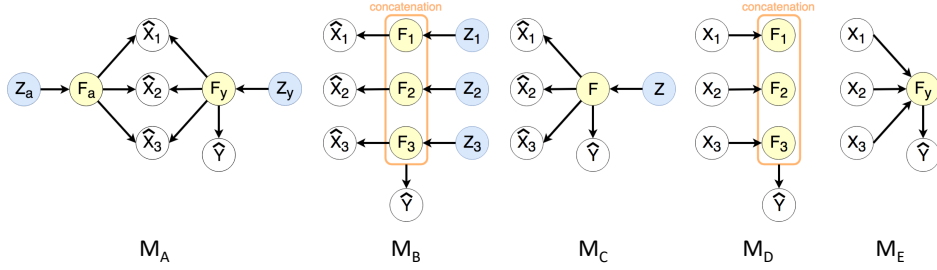


Figure 6: Models used in the ablation studies of MFM. Each model removes a design component (Table 2).

icates greater contribution from  $F_y$  to  $\hat{X}_i$ . We compare ratios  $r_i = \text{Depen}(F_y, \hat{X}_i) / \text{Depen}(F_{a_i}, \hat{X}_i)$  to measure a normalized version w.r.t. the dependency measure between  $F_{a_i}$  and  $\hat{X}_i$ . The normalized Hilbert-Schmidt Independence Criterion [17; 63] is chosen as our dependency measure:

$$\text{Depen}(F, \hat{X}_i) = \text{HSIC}_{norm}(F, \hat{X}_i) = \frac{\text{tr}(\mathbf{K}_F \mathbf{H} \mathbf{K}_{\hat{X}_i} \mathbf{H})}{\|\mathbf{H} \mathbf{K}_F \mathbf{H}\|_F \|\mathbf{H} \mathbf{K}_{\hat{X}_i} \mathbf{H}\|_F}, \quad (5)$$

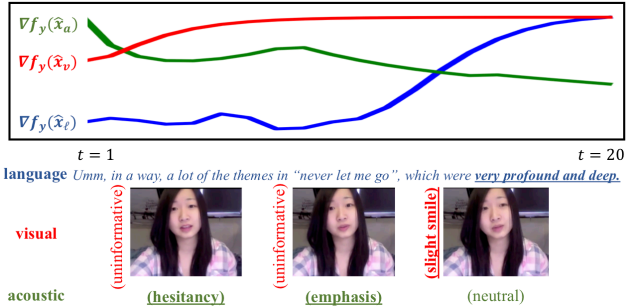
where  $\cdot$  represents  $y$  or  $a_i$ ,  $n$  is the number of  $\{F, \hat{X}_i\}$  pairs,  $\mathbf{H} = \mathbf{I} - \frac{1}{n} \mathbf{1} \mathbf{1}^\top$ ,  $\mathbf{K}_F \in \mathbb{R}^{n \times n}$  is the Gram matrix of  $F$ . with  $\mathbf{K}_{F,ij} = k_1(F_i, F_j)$ ,  $\mathbf{K}_{\hat{X}_i} \in \mathbb{R}^{n \times n}$  is the Gram matrix of  $\hat{X}_i$  with  $\mathbf{K}_{\hat{X}_i,jk} = k_2(\hat{X}_{ij}, \hat{X}_{ik})$ .  $k_1(\cdot, \cdot)$  and  $k_2(\cdot, \cdot)$  are predefined kernel functions (details in supplementary).

Figure 9 (a) shows the results for two multimodal datasets, CMU-MOSI and POM. We observe that on CMU-MOSI, the language modality is most informative towards sentiment predictions, followed by the acoustic modality. This result represents a prior over the expression of sentiment in human multimodal language and is closely related to the connections between language and speech [25].

For multimodal personality trait recognition on the POM dataset, we observe that the language modality is also the most informative while the visual and acoustic modalities are almost equally informative. This result is in agreement with behavioral studies which have observed that non-verbal behaviors are particularly informative of personality traits [18; 29; 32]. For example, the same sentence “this movie was great” can convey significantly different messages on speaker confidence depending on whether it was said in a loud and exciting voice, with eye contact, or powerful gesticulation.

Ratio	$r_\ell$ (language)	$r_v$ (visual)	$r_a$ (acoustic)
CMU-MOSI	0.307	0.030	0.107
POM	1.090	0.996	0.898

(a) Dependency-based interpretation on CMU-MOSI and POM.



(b) Gradient-based interpretation on CMU-MOSI videos.

Figure 9: Analyzing the multimodal representations learnt in MFM via (a) dependency-based and (b) gradient-based interpretation methods. For the gradient-based interpretations, bolded behaviors “very profound and deep” in the language modality, slight smile in the visual modality as well as hesitant and emphasized tone of voice in the acoustic modality correspond to increases in  $\nabla_{f_y}(\hat{x}_i)$ .

**Gradient-based Interpretation:** The gradient-based interpretation assesses the contributions of each modality at a fine-grained resolution (i.e., for every time step in a time series). The intuition is that measuring the gradient of the generated modality with respect to target factors (e.g.,  $\mathbf{F}_y$ ) allows us to analyze how the factor influences generation of individual modalities. Let  $\{x_1, x_2, \dots, x_M\}$  denote multimodal time series data where  $x_i$  represents modality  $i$ . MFM reconstructs  $x_i$  as follows:

$$\hat{x}_i = F_i(f_{ai}, f_y), f_{ai} = G_{ai}(z_{ai}), f_y = G_y(z_y), z_{ai} \sim Q(\mathbf{Z}_{ai} | \mathbf{X}_i = x_i), z_y \sim Q(\mathbf{Z}_y | \mathbf{X}_{1:M} = x_{1:M}). \quad (6)$$

In Equation (6),  $\hat{x}_i = [\hat{x}_i^1, \dots, \hat{x}_i^t, \dots, \hat{x}_i^T]$  with time step  $t \in [1, T]$ . We define the gradient norm flow through time as follows:

$$\nabla_{f_y}(\hat{x}_i) := [\|\nabla_{f_y} \hat{x}_i^1\|_F^2, \|\nabla_{f_y} \hat{x}_i^2\|_F^2, \dots, \|\nabla_{f_y} \hat{x}_i^T\|_F^2] \quad (7)$$

where  $\nabla_{f_y}(\hat{x}_i)$  measures the extent to which changes in  $f_y$  influences the generation of sequence  $\hat{x}_i$ . In Figure 9 (b), we plot  $\nabla_{f_y}(\hat{x}_i)$  over time for a video in the CMU-MOSI dataset. We observe that multimodal communicative behaviors that are strongly indicative of speaker sentiment such as positive words (e.g. “very profound and deep”) and informative acoustic features (e.g. hesitant and emphasized tone of voice) indeed correspond to increases in  $\nabla_{f_y}(\hat{x}_i)$ .

## 4 Related Work

The two main pillars of research in multimodal representation learning have considered the discriminative and generative objectives individually. Discriminative representation learning [65; 8; 7; 14; 51; 59; 58] models the conditional distribution  $P(\mathbf{Y} | \mathbf{X}_{1:M})$  to predict  $\mathbf{Y}$  given  $\mathbf{X}_{1:M}$ . Since these approaches are not concerned with modeling  $P(\mathbf{X}_{1:M})$  explicitly, they use parameters more efficiently to model  $P(\mathbf{Y} | \mathbf{X}_{1:M})$ . For instance, recent works learn visual representations that are maximally dependent with linguistic attributes for improving one-shot image recognition [59] or introduce tensor product mechanisms to model interactions between the language, visual and acoustic modalities [65]. Learning discriminative representations preserves task-relevant features while task-irrelevant features may be discarded. On the other hand, generative representation learning [36; 55; 56] captures the interactions between modalities by modeling the joint distribution  $P(\mathbf{X}_1, \dots, \mathbf{X}_M)$  using either undirected graphical models [55], directed graphical models [56], or neural networks [52]. Some generative approaches for representation learning compress multimodal information into a single feature vector with lower dimensions than the original data, which can be an advantage when later used for discriminative tasks [36; 55; 56]. Generative and discriminative approaches each bring important properties for multimodal representation learning. Our proposed MFM approach combines the advantages of both discriminative and generative properties.

Factorized representation learning resembles learning disentangled data representations [4; 26; 27; 9; 19; 49]. Disentangled representations have been shown to improve the performance on artificial intelligence tasks [4; 27; 23; 64; 10; 48; 69]. Several methods involve specifying a fixed set of latent attributes that individually control particular variations of data and performing supervised training [10; 23; 64; 48; 69], assuming an isotropic Gaussian prior over latent variables to learn disentangled generative representations [24; 19; 49] and learning latent variables in charge of specific variations in the data by maximizing the mutual information between a subset of latent variables and the data [9]. However, these methods study factorized representations in a single modality. MFM factorizes multimodal representations into independent factors while keeping the unity of modality-specific and multimodal factors.

## 5 Conclusion and Future Work

In this paper, we propose the Multimodal Factorization Model (MFM) for multimodal representation learning. MFM factorizes the multimodal representations into two sets of independent factors: *multimodal discriminative* factors and *modality-specific generative* factors. The multimodal discriminative factor achieves state-of-the-art or competitive results on five multimodal datasets. At the same time, the modality-specific generative factors allow us to generate data based on factorized variables and have a deeper understanding of the interactions involved in multimodal learning. Our future work will explore extensions of MFM for multimodal time series generation (i.e., video generation), semi-supervised or unsupervised learning, and cross-modal adaptation (i.e., modality translation). We believe that MFM sheds light on the advantages of factorizing multimodal representations and potentially opens up new horizons for novel applications of multimodal machine learning.



## References

- [1] Fernando Alonso-Martin, Maria Malfaz, Joao Sequeira, Javier F. Gorostiza, and Miguel A. Salichs. A multimodal emotion detection system during human-robot interaction. *Sensors*, 13(11):15549–15581, 2013.
- [2] Tadas Baltrušaitis, Chaitanya Ahuja, and Louis-Philippe Morency. Multimodal machine learning: A survey and taxonomy. *CoRR*, abs/1705.09406, 2017.
- [3] Tadas Baltrušaitis, Chaitanya Ahuja, and Louis-Philippe Morency. Multimodal machine learning: A survey and taxonomy. *arXiv preprint arXiv:1705.09406*, 2017.
- [4] Yoshua Bengio, Aaron Courville, and Pascal Vincent. Representation learning: A review and new perspectives. *IEEE Trans. Pattern Anal. Mach. Intell.*, 35(8):1798–1828, August 2013.
- [5] Leo Breiman. Random forests. *Mach. Learn.*, 45(1):5–32, October 2001.
- [6] Carlos Busso, Murtaza Bulut, Chi-Chun Lee, Abe Kazemzadeh, Emily Mower, Samuel Kim, Jeannette Chang, Sungbok Lee, and Shrikanth S. Narayanan. Iemocap: Interactive emotional dyadic motion capture database. *Journal of Language Resources and Evaluation*, 42(4):335–359, dec 2008.
- [7] Devendra Singh Chaplot, Kanthashree Mysore Sathyendra, Rama Kumar Pasumarthi, Dheeraj Rajagopal, and Ruslan Salakhutdinov. Gated-attention architectures for task-oriented language grounding. *arXiv preprint arXiv:1706.07230*, 2017.
- [8] Minghai Chen, Sen Wang, Paul Pu Liang, Tadas Baltrušaitis, Amir Zadeh, and Louis-Philippe Morency. Multimodal sentiment analysis with word-level fusion and reinforcement learning. In *Proceedings of the 19th ACM International Conference on Multimodal Interaction, ICMI 2017*, 2017.
- [9] Xi Chen, Yan Duan, Rein Houthoofd, John Schulman, Ilya Sutskever, and Pieter Abbeel. Infogan: Interpretable representation learning by information maximizing generative adversarial nets. In *Advances in Neural Information Processing Systems*, pages 2172–2180, 2016.
- [10] Brian Cheung, Jesse A Livezey, Arjun K Bansal, and Bruno A Olshausen. Discovering hidden factors of variation in deep networks. *arXiv preprint arXiv:1412.6583*, 2014.
- [11] Kyunghyun Cho, Bart van Merriënboer, Çağlar Gülçehre, Dzmitry Bahdanau, Fethi Bougares, Holger Schwenk, and Yoshua Bengio. Learning phrase representations using rnn encoder–decoder for statistical machine translation. In *Proceedings of the 2014 Conference on Empirical Methods in Natural Language Processing (EMNLP)*, pages 1724–1734, Doha, Qatar, October 2014. Association for Computational Linguistics.
- [12] Gilles Degottex, John Kane, Thomas Drugman, Tuomo Raitio, and Stefan Scherer. Covarepa collaborative voice analysis repository for speech technologies. In *Acoustics, Speech and Signal Processing (ICASSP), 2014 IEEE International Conference on*, pages 960–964. IEEE, 2014.
- [13] C. A. Frantzidis, C. Bratsas, M. A. Klados, E. Konstantinidis, C. D. Lithari, A. B. Vivas, C. L. Papadelis, E. Kaldoudi, C. Pappas, and P. D. Bamidis. On the classification of emotional biosignals evoked while viewing affective pictures: An integrated data-mining-based approach for healthcare applications. *IEEE Transactions on Information Technology in Biomedicine*, 14(2):309–318, March 2010.
- [14] Andrea Frome, Greg S Corrado, Jon Shlens, Samy Bengio, Jeff Dean, Tomas Mikolov, et al. Devise: A deep visual-semantic embedding model. In *Advances in neural information processing systems*, pages 2121–2129, 2013.
- [15] A. Graves, A. r. Mohamed, and G. Hinton. Speech recognition with deep recurrent neural networks. In *2013 IEEE International Conference on Acoustics, Speech and Signal Processing*, pages 6645–6649, May 2013.
- [16] Arthur Gretton, Karsten M Borgwardt, Malte J Rasch, Bernhard Schölkopf, and Alexander Smola. A kernel two-sample test. *Journal of Machine Learning Research*, 13(Mar):723–773, 2012.

- [17] Arthur Gretton, Olivier Bousquet, Alex Smola, and Bernhard Schölkopf. Measuring statistical dependence with hilbert-schmidt norms. In *International conference on algorithmic learning theory*, pages 63–77. Springer, 2005.
- [18] Sylvain Guimond and Wael Massrieh. Intricate correlation between body posture, personality trait and incidence of body pain: A cross-referential study report. *PLOS ONE*, 7(5):1–8, 05 2012.
- [19] Irina Higgins, Loic Matthey, Arka Pal, Christopher Burgess, Xavier Glorot, Matthew Botvinick, Shakir Mohamed, and Alexander Lerchner. beta-vae: Learning basic visual concepts with a constrained variational framework. 2016.
- [20] Sepp Hochreiter and Jürgen Schmidhuber. Long short-term memory. *Neural Comput.*, 9(8):1735–1780, November 1997.
- [21] Sepp Hochreiter and Jürgen Schmidhuber. Long short-term memory. *Neural computation*, 9(8):1735–1780, 1997.
- [22] iMotions. Facial expression analysis, 2017.
- [23] Theofanis Karaletsos, Serge Belongie, and Gunnar Rätsch. Bayesian representation learning with oracle constraints. *arXiv preprint arXiv:1506.05011*, 2015.
- [24] Diederik P Kingma and Max Welling. Auto-encoding variational bayes. *arXiv preprint arXiv:1312.6114*, 2013.
- [25] Patricia K. Kuhl. A new view of language acquisition. *Proceedings of the National Academy of Sciences*, 97(22):11850–11857, 2000.
- [26] Tejas D Kulkarni, William F Whitney, Pushmeet Kohli, and Josh Tenenbaum. Deep convolutional inverse graphics network. In *Advances in Neural Information Processing Systems*, pages 2539–2547, 2015.
- [27] Brenden M Lake, Tomer D Ullman, Joshua B Tenenbaum, and Samuel J Gershman. Building machines that learn and think like people. *Behavioral and Brain Sciences*, 40, 2017.
- [28] Yann Lecun, Léon Bottou, Yoshua Bengio, and Patrick Haffner. Gradient-based learning applied to document recognition. In *Proceedings of the IEEE*, pages 2278–2324, 1998.
- [29] Sergey Levine, Christian Theobalt, and Vladlen Koltun. Real-time prosody-driven synthesis of body language. *ACM Trans. Graph.*, 28(5):172:1–172:10, December 2009.
- [30] Z. Liu, M. Wu, W. Cao, L. Chen, J. Xu, R. Zhang, M. Zhou, and J. Mao. A facial expression emotion recognition based human-robot interaction system. *IEEE/CAA Journal of Automatica Sinica*, 4(4):668–676, 2017.
- [31] Mehdi Malekzadeh, Mumtaz Begum Mustafa, and Adel Lahsasna. A review of emotion regulation in intelligent tutoring systems. *Journal of Educational Technology and Society*, 18(4):435–445, 2015.
- [32] Gelareh Mohammadi, Alessandro Vinciarelli, and Marcello Mortillaro. The voice of personality: Mapping nonverbal vocal behavior into trait attributions. In *Proceedings of ACM Multimedia Workshop on Social Signal Processing*, 0 2010.
- [33] Louis-Philippe Morency, Rada Mihalcea, and Payal Doshi. Towards multimodal sentiment analysis: Harvesting opinions from the web. In *Proceedings of the 13th international conference on multimodal interfaces*, pages 169–176. ACM, 2011.
- [34] Louis-Philippe Morency, Ariadna Quattoni, and Trevor Darrell. Latent-dynamic discriminative models for continuous gesture recognition. In *Computer Vision and Pattern Recognition, 2007. CVPR’07. IEEE Conference on*, pages 1–8. IEEE, 2007.
- [35] Yuval Netzer, Tao Wang, Adam Coates, Alessandro Bissacco, Bo Wu, and Andrew Y. Ng. Reading digits in natural images with unsupervised feature learning. 2011.

- [36] Jiquan Ngiam, Aditya Khosla, Mingyu Kim, Juhan Nam, Honglak Lee, and Andrew Y Ng. Multimodal deep learning. In *Proceedings of the 28th international conference on machine learning (ICML-11)*, pages 689–696, 2011.
- [37] Behnaz Nojavanasghari, Deepak Gopinath, Jayanth Koushik, Tadas Baltrušaitis, and Louis-Philippe Morency. Deep multimodal fusion for persuasiveness prediction. In *Proceedings of the 18th ACM International Conference on Multimodal Interaction, ICMI 2016*, pages 284–288, New York, NY, USA, 2016. ACM.
- [38] Behnaz Nojavanasghari, Charles E. Hughes, and Louis-Philippe Morency. Exceptionally social: Design of an avatar-mediated interactive system for promoting social skills in children with autism. In *Proceedings of the 2017 CHI Conference Extended Abstracts on Human Factors in Computing Systems, CHI EA '17*, pages 1932–1939, New York, NY, USA, 2017. ACM.
- [39] Sunghyun Park, Han Suk Shim, Moitreyia Chatterjee, Kenji Sagae, and Louis-Philippe Morency. Computational analysis of persuasiveness in social multimedia: A novel dataset and multimodal prediction approach. In *Proceedings of the 16th International Conference on Multimodal Interaction, ICMI '14*, pages 50–57, New York, NY, USA, 2014. ACM.
- [40] Jeffrey Pennington, Richard Socher, and Christopher D Manning. Glove: Global vectors for word representation. In *EMNLP*, volume 14, pages 1532–1543, 2014.
- [41] Sintija Petrovica, Alla Anohina-Naumeca, and HazÄ±m Kemal Ekenel. Emotion recognition in affective tutoring systems: Collection of ground-truth data. *Procedia Computer Science*, 104:437 – 444, 2017. ICTE 2016, Riga Technical University, Latvia.
- [42] Johannes Pittermann, Angela Pittermann, and Wolfgang Minker. *Handling Emotions in Human-Computer Dialogues*. Springer Publishing Company, Incorporated, 1st edition, 2009.
- [43] Johannes Pittermann, Angela Pittermann, and Wolfgang Minker. Emotion recognition and adaptation in spoken dialogue systems. *International Journal of Speech Technology*, 13(1):49–60, Mar 2010.
- [44] Soujanya Poria, Erik Cambria, and Alexander Gelbukh. Deep convolutional neural network textual features and multiple kernel learning for utterance-level multimodal sentiment analysis. In *Proceedings of the 2015 Conference on Empirical Methods in Natural Language Processing*, pages 2539–2544, 2015.
- [45] Soujanya Poria, Erik Cambria, Devamanyu Hazarika, Navonil Majumder, Amir Zadeh, and Louis-Philippe Morency. Context-dependent sentiment analysis in user-generated videos. In *Proceedings of the 55th Annual Meeting of the Association for Computational Linguistics (Volume 1: Long Papers)*, volume 1, pages 873–883, 2017.
- [46] Ariadna Quattoni, Sybor Wang, Louis-Philippe Morency, Michael Collins, and Trevor Darrell. Hidden conditional random fields. *IEEE Trans. Pattern Anal. Mach. Intell.*, 29(10):1848–1852, October 2007.
- [47] Shyam Sundar Rajagopalan, Louis-Philippe Morency, Tadas Baltrušaitis, and Goecke Roland. Extending long short-term memory for multi-view structured learning. In *European Conference on Computer Vision*, 2016.
- [48] Scott Reed, Kihyuk Sohn, Yuting Zhang, and Honglak Lee. Learning to disentangle factors of variation with manifold interaction. In *International Conference on Machine Learning*, pages 1431–1439, 2014.
- [49] Paul K Rubenstein, Bernhard Schoelkopf, and Ilya Tolstikhin. On the latent space of wasserstein auto-encoders. *arXiv preprint arXiv:1802.03761*, 2018.
- [50] M. Schuster and K.K. Paliwal. Bidirectional recurrent neural networks. *Trans. Sig. Proc.*, 45(11):2673–2681, November 1997.
- [51] Richard Socher, Milind Ganjoo, Christopher D Manning, and Andrew Ng. Zero-shot learning through cross-modal transfer. In *Advances in neural information processing systems*, pages 935–943, 2013.

- [52] Kihyuk Sohn, Wenling Shang, and Honglak Lee. Improved multimodal deep learning with variation of information. In *Advances in Neural Information Processing Systems*, pages 2141–2149, 2014.
- [53] Yale Song, Louis-Philippe Morency, and Randall Davis. Multi-view latent variable discriminative models for action recognition. In *Computer Vision and Pattern Recognition (CVPR), 2012 IEEE Conference on*, pages 2120–2127. IEEE, 2012.
- [54] Yale Song, Louis-Philippe Morency, and Randall Davis. Action recognition by hierarchical sequence summarization. In *Proceedings of the IEEE Conference on Computer Vision and Pattern Recognition*, pages 3562–3569, 2013.
- [55] Nitish Srivastava and Ruslan R Salakhutdinov. Multimodal learning with deep boltzmann machines. In *Advances in neural information processing systems*, pages 2222–2230, 2012.
- [56] Masahiro Suzuki, Kotaro Nakayama, and Yutaka Matsuo. Joint multimodal learning with deep generative models. *arXiv preprint arXiv:1611.01891*, 2016.
- [57] Ilya Tolstikhin, Olivier Bousquet, Sylvain Gelly, and Bernhard Schoelkopf. Wasserstein auto-encoders. *arXiv preprint arXiv:1711.01558*, 2017.
- [58] Yao-Hung Hubert Tsai, Liang-Kang Huang, and Ruslan Salakhutdinov. Learning robust visual-semantic embeddings. *arXiv preprint arXiv:1703.05908*, 2017.
- [59] Yao-Hung Hubert Tsai and Ruslan Salakhutdinov. Improving one-shot learning through fusing side information. *arXiv preprint arXiv:1710.08347*, 2017.
- [60] Alexandria K. Vail, Joseph F. Grafsgaard, Kristy Elizabeth Boyer, Eric N. Wiebe, and James C. Lester. Gender differences in facial expressions of affect during learning. In *Proceedings of the 2016 Conference on User Modeling Adaptation and Personalization, UMAP '16*, pages 65–73, New York, NY, USA, 2016. ACM.
- [61] Haohan Wang, Aaksha Meghawat, Louis-Philippe Morency, and Eric P Xing. Select-additive learning: Improving cross-individual generalization in multimodal sentiment analysis. *arXiv preprint arXiv:1609.05244*, 2016.
- [62] Martin Wöllmer, Felix Weninger, Tobias Knaup, Björn Schuller, Congkai Sun, Kenji Sagae, and Louis-Philippe Morency. Youtube movie reviews: Sentiment analysis in an audio-visual context. *IEEE Intelligent Systems*, 28(3):46–53, 2013.
- [63] Denny Wu, Yixiu Zhao, Yao-Hung Hubert Tsai, Makoto Yamada, and Ruslan Salakhutdinov. "dependency bottleneck" in auto-encoding architectures: an empirical study. *arXiv preprint arXiv:1802.05408*, 2018.
- [64] Jimei Yang, Scott E Reed, Ming-Hsuan Yang, and Honglak Lee. Weakly-supervised disentangling with recurrent transformations for 3d view synthesis. In *Advances in Neural Information Processing Systems*, pages 1099–1107, 2015.
- [65] Amir Zadeh, Minghai Chen, Soujanya Poria, Erik Cambria, and Louis-Philippe Morency. Tensor fusion network for multimodal sentiment analysis. In *Empirical Methods in Natural Language Processing, EMNLP*, 2017.
- [66] Amir Zadeh, Paul Pu Liang, Navonil Mazumder, Soujanya Poria, Erik Cambria, and Louis-Philippe Morency. Memory fusion network for multi-view sequential learning. *Proceedings of the Thirty-Second AAAI Conference on Artificial Intelligence*, 2018.
- [67] Amir Zadeh, Paul Pu Liang, Soujanya Poria, Prateek Vij, Erik Cambria, and Louis-Philippe Morency. Multi-attention recurrent network for human communication comprehension. *Proceedings of the Thirty-Second AAAI Conference on Artificial Intelligence*, 2018.
- [68] Amir Zadeh, Rowan Zellers, Eli Pincus, and Louis-Philippe Morency. Multimodal sentiment intensity analysis in videos: Facial gestures and verbal messages. *IEEE Intelligent Systems*, 31(6):82–88, 2016.

- [69] Zhenyao Zhu, Ping Luo, Xiaogang Wang, and Xiaoou Tang. Multi-view perceptron: a deep model for learning face identity and view representations. In *Advances in Neural Information Processing Systems*, pages 217–225, 2014.

# Supplementary for Learning Factorized Multimodal Representations

Yao-Hung Hubert Tsai <sup>\*1</sup> Paul Pu Liang <sup>\*1</sup>

Amir Zadeh <sup>2</sup> Louis-Philippe Morency <sup>2</sup> Ruslan Salakhutdinov <sup>1</sup>

Machine Learning Department<sup>1</sup> Language Technologies Institute<sup>2</sup>, Carnegie Mellon University  
 {yaohungt, pli, abagherz, morency, rsalakhu}@cs.cmu.edu

## A Proof of Proposition 1

To simplify the proof, we first prove it for the unimodal case. That is, we aim to prove the Wasserstein distance between  $P_{\mathbf{X}, \mathbf{Y}}$  and  $P_{\hat{\mathbf{X}}, \hat{\mathbf{Y}}}$ .

### A.A Unimodal Joint-Distribution Wasserstein Distance

**Proposition 1.** For any functions  $G_y : \mathbf{Z}_y \rightarrow \mathbf{F}_y$ ,  $G_a : \mathbf{Z}_a \rightarrow \mathbf{F}_a$ ,  $D : \mathbf{F}_y \rightarrow \hat{\mathbf{Y}}$ , and  $F : \mathbf{F}_a, \mathbf{F}_y \rightarrow \hat{\mathbf{X}}$ , we have

$$W_c(P_{\mathbf{X}, \mathbf{Y}}, P_{\hat{\mathbf{X}}, \hat{\mathbf{Y}}}) = \inf_{Q_{\mathbf{Z}}=P_{\mathbf{Z}}} \mathbf{E}_{P_{\mathbf{X}, \mathbf{Y}}} \mathbf{E}_{Q_{\mathbf{Z}}(\mathbf{Z}|\mathbf{X})} \left[ c_X(\mathbf{X}, F(G_a(\mathbf{Z}_a), G_y(\mathbf{Z}_y))) + c_Y(\mathbf{Y}, D(G_y(\mathbf{Z}_y))) \right], \quad (1)$$

where  $W_c$  is the Wasserstein distance under cost function  $c_X$  and  $c_Y$ ,  $P_{\mathbf{Z}}$  is the prior over  $\mathbf{Z} = [\mathbf{Z}_a, \mathbf{Z}_y]$  and  $Q_{\mathbf{Z}}$  is the aggregated posterior of the proposed inference distribution  $Q(\mathbf{Z}|\mathbf{X})$ .

*Proof:* See the following.

To begin the proof, we abuse some notations as follows.

By definition, the Wasserstein distance under cost function  $c$  between  $P_{\mathbf{X}, \mathbf{Y}}$  and  $P_{\hat{\mathbf{X}}, \hat{\mathbf{Y}}}$  is

$$W_c(P_{\mathbf{X}, \mathbf{Y}}, P_{\hat{\mathbf{X}}, \hat{\mathbf{Y}}}) := \inf_{\Gamma \in \mathcal{P}((\mathbf{X}, \mathbf{Y}) \sim P_{\mathbf{X}, \mathbf{Y}}, (\hat{\mathbf{X}}, \hat{\mathbf{Y}}) \sim P_{\hat{\mathbf{X}}, \hat{\mathbf{Y}}})} \mathbf{E}_{(\mathbf{X}, \mathbf{Y}), (\hat{\mathbf{X}}, \hat{\mathbf{Y}}) \sim \Gamma} [c((\mathbf{X}, \mathbf{Y}), (\hat{\mathbf{X}}, \hat{\mathbf{Y}}))], \quad (2)$$

where  $c((\mathbf{X}, \mathbf{Y}), (\hat{\mathbf{X}}, \hat{\mathbf{Y}})) : (\mathcal{X}, \mathcal{Y}) \times (\mathcal{X}, \mathcal{Y}) \rightarrow \mathcal{R}_+$  is any measurable *cost function*.  $\mathcal{P}((\mathbf{X}, \mathbf{Y}) \sim P_{\mathbf{X}, \mathbf{Y}}, (\hat{\mathbf{X}}, \hat{\mathbf{Y}}) \sim P_{\hat{\mathbf{X}}, \hat{\mathbf{Y}}})$  is the set of all joint distributions of  $((\mathbf{X}, \mathbf{Y}), (\hat{\mathbf{X}}, \hat{\mathbf{Y}}))$  with marginals  $P_{\mathbf{X}, \mathbf{Y}}$  and  $P_{\hat{\mathbf{X}}, \hat{\mathbf{Y}}}$ , respectively. Note that  $c((\mathbf{X}, \mathbf{Y}), (\hat{\mathbf{X}}, \hat{\mathbf{Y}})) = c_X(\mathbf{X}, \hat{\mathbf{X}}) + c_Y(\mathbf{Y}, \hat{\mathbf{Y}})$ .

Next, we denote the set of all joint distributions of  $(\mathbf{X}, \mathbf{Y}, \hat{\mathbf{X}}, \hat{\mathbf{Y}}, \mathbf{Z})$  such that  $(\mathbf{X}, \mathbf{Y}) \sim P_{\mathbf{X}, \mathbf{Y}}$ ,  $(\hat{\mathbf{X}}, \hat{\mathbf{Y}}, \mathbf{Z}) \sim P_{\hat{\mathbf{X}}, \hat{\mathbf{Y}}, \mathbf{Z}}$ , and  $((\mathbf{X}, \mathbf{Y}) \perp (\hat{\mathbf{X}}, \hat{\mathbf{Y}})|\mathbf{Z})$  as  $\mathcal{P}_{\mathbf{X}, \mathbf{Y}, \hat{\mathbf{X}}, \hat{\mathbf{Y}}, \mathbf{Z}}$ .  $\mathcal{P}_{\mathbf{X}, \mathbf{Y}, \hat{\mathbf{X}}, \hat{\mathbf{Y}}}$  and  $\mathcal{P}_{\mathbf{X}, \mathbf{Y}, \mathbf{Z}}$  are the sets of the marginals  $(\mathbf{X}, \mathbf{Y}, \hat{\mathbf{X}}, \hat{\mathbf{Y}})$  and  $(\mathbf{X}, \mathbf{Y}, \mathbf{Z})$  induced by  $\mathcal{P}_{\mathbf{X}, \mathbf{Y}, \hat{\mathbf{X}}, \hat{\mathbf{Y}}, \mathbf{Z}}$ .

Then, we introduce two Lemmas to help the proof.

**Lemma 1.**  $P(\hat{\mathbf{X}}, \hat{\mathbf{Y}}|\mathbf{Z} = z)$  are Dirac for all  $z \in \mathcal{Z}$ .

*Proof:* First, we have  $\hat{\mathbf{X}} = F(G_a(\mathbf{Z}_a), G_y(\mathbf{Z}_y))$  and  $\hat{\mathbf{Y}} = D(G_y(\mathbf{Z}_y))$  with  $\mathbf{Z} = \{\mathbf{Z}_a, \mathbf{Z}_y\}$ . Since the functions  $F, G_a, G_y, D$  are all deterministic, then  $P(\hat{\mathbf{X}}, \hat{\mathbf{Y}}|\mathbf{Z})$  are Dirac measures.  $\square$

<sup>\*</sup>equal contributions

**Lemma 2.**  $\mathcal{P}(P_{\mathbf{X}, \mathbf{Y}}, P_{\hat{\mathbf{X}}, \hat{\mathbf{Y}}}) = \mathcal{P}_{\mathbf{X}, \mathbf{Y}, \hat{\mathbf{X}}, \hat{\mathbf{Y}}}$  when  $P(\hat{\mathbf{X}}, \hat{\mathbf{Y}}|\mathbf{Z} = z)$  are Dirac for all  $z \in \mathcal{Z}$ .

*Proof:* When  $\hat{\mathbf{X}}, \hat{\mathbf{Y}}$  are deterministic functions of  $\mathbf{Z}$ , for any  $A$  in the sigma-algebra induced by  $\hat{\mathbf{X}}, \hat{\mathbf{Y}}$ , we have

$$\mathbf{E}[\mathbb{I}_{[\hat{\mathbf{X}}, \hat{\mathbf{Y}} \in A]}|\mathbf{X}, \mathbf{Y}, \mathbf{Z}] = \mathbf{E}[\mathbb{I}_{[\hat{\mathbf{X}}, \hat{\mathbf{Y}} \in A]}|\mathbf{Z}].$$

Therefore, this implies that  $(\mathbf{X}, \mathbf{Y}) \perp (\hat{\mathbf{X}}, \hat{\mathbf{Y}})|\mathbf{Z}$  which concludes the proof. A similar argument is made in Lemma 1 of [16].

□

Now, we use the fact that  $\mathcal{P}(P_{\mathbf{X}, \mathbf{Y}}, P_{\hat{\mathbf{X}}, \hat{\mathbf{Y}}}) = \mathcal{P}_{\mathbf{X}, \mathbf{Y}, \hat{\mathbf{X}}, \hat{\mathbf{Y}}}$  (Lemma 1 + Lemma 2),  $c((\mathbf{X}, \mathbf{Y}), (\hat{\mathbf{X}}, \hat{\mathbf{Y}})) = c_X(\mathbf{X}, \hat{\mathbf{X}}) + c_Y(\mathbf{Y}, \hat{\mathbf{Y}})$ ,  $\hat{\mathbf{X}} = F(G_a(\mathbf{Z}_a), G_y(\mathbf{Z}_y))$ , and  $\hat{\mathbf{Y}} = D(G_y(\mathbf{Z}_y))$ , Eq. (2) becomes

$$\begin{aligned} & \inf_{P \in \mathcal{P}_{\mathbf{X}, \mathbf{Y}, \hat{\mathbf{X}}, \hat{\mathbf{Y}}}} \mathbf{E}_{\mathbf{X}, \mathbf{Y}, \hat{\mathbf{X}}, \hat{\mathbf{Y}} \sim P} [c_X(\mathbf{X}, \hat{\mathbf{X}}) + c_Y(\mathbf{Y}, \hat{\mathbf{Y}})] \\ &= \inf_{P \in \mathcal{P}_{\mathbf{X}, \mathbf{Y}, \hat{\mathbf{X}}, \hat{\mathbf{Y}}, \mathbf{Z} \sim P}} \mathbf{E}_{\mathbf{X}, \mathbf{Y}, \hat{\mathbf{X}}, \hat{\mathbf{Y}}, \mathbf{Z} \sim P} [c_X(\mathbf{X}, \hat{\mathbf{X}}) + c_Y(\mathbf{Y}, \hat{\mathbf{Y}})] \\ &= \inf_{P \in \mathcal{P}_{\mathbf{X}, \mathbf{Y}, \hat{\mathbf{X}}, \hat{\mathbf{Y}}, \mathbf{Z}}} \mathbf{E}_{P_Z} \mathbf{E}_{P(\mathbf{X}, \mathbf{Y}|\mathbf{Z})} \mathbf{E}_{P(\hat{\mathbf{X}}, \hat{\mathbf{Y}}|\mathbf{Z})} [c_X(\mathbf{X}, \hat{\mathbf{X}}) + c_Y(\mathbf{Y}, \hat{\mathbf{Y}})] \\ &= \inf_{P \in \mathcal{P}_{\mathbf{X}, \mathbf{Y}, \hat{\mathbf{X}}, \hat{\mathbf{Y}}, \mathbf{Z}}} \mathbf{E}_{P_Z} \mathbf{E}_{P(\mathbf{X}, \mathbf{Y}|\mathbf{Z})} [c_X(\mathbf{X}, F(G_a(\mathbf{Z}_a), G_y(\mathbf{Z}_y))) + c_Y(\mathbf{Y}, D(G_y(\mathbf{Z}_y)))] \\ &= \inf_{P \in \mathcal{P}_{\mathbf{X}, \mathbf{Y}, \mathbf{Z}}} \mathbf{E}_{P_Z} \mathbf{E}_{P(\mathbf{X}, \mathbf{Y}|\mathbf{Z})} [c_X(\mathbf{X}, F(G_a(\mathbf{Z}_a), G_y(\mathbf{Z}_y))) + c_Y(\mathbf{Y}, D(G_y(\mathbf{Z}_y)))] \\ &= \inf_{P \in \mathcal{P}_{\mathbf{X}, \mathbf{Y}, \mathbf{Z}}} \mathbf{E}_{\mathbf{X}, \mathbf{Y}, \mathbf{Z} \sim P} [c_X(\mathbf{X}, F(G_a(\mathbf{Z}_a), G_y(\mathbf{Z}_y))) + c_Y(\mathbf{Y}, D(G_y(\mathbf{Z}_y)))] \end{aligned} \quad (3)$$

Note that in Eq. (3),  $\mathcal{P}_{\mathbf{X}, \mathbf{Y}, \mathbf{Z}} = \mathcal{P}((\mathbf{X}, \mathbf{Y}) \sim P_{\mathbf{X}, \mathbf{Y}}, \mathbf{Z} \sim P_Z)$  and with a proposed  $Q(\mathbf{Z}|\mathbf{X})$ , we can rewrite Eq. (3) as

$$\begin{aligned} & \inf_{P \in \mathcal{P}_{\mathbf{X}, \mathbf{Y}, \mathbf{Z}}} \mathbf{E}_{P_{\mathbf{X}, \mathbf{Y}}} \mathbf{E}_{P_Z} [c_X(\mathbf{X}, F(G_a(\mathbf{Z}_a), G_y(\mathbf{Z}_y))) + c_Y(\mathbf{Y}, D(G_y(\mathbf{Z}_y)))] \\ &= \inf_{Q_Z = P_Z} \mathbf{E}_{P_{\mathbf{X}, \mathbf{Y}}} \mathbf{E}_{Q(\mathbf{Z}|\mathbf{X})} \left[ c_X(\mathbf{X}, F(G_a(\mathbf{Z}_a), G_y(\mathbf{Z}_y))) + c_Y(\mathbf{Y}, D(G_y(\mathbf{Z}_y))) \right] \end{aligned} \quad (4)$$

■

## A.B From Unimodal to Multimodal

The proof is similar to Proposition 1, and we present a sketch to it. We can first show  $P(\hat{\mathbf{X}}_{1:M}, \hat{\mathbf{Y}}|\mathbf{Z} = z)$  are Dirac for all  $z \in \mathcal{Z}$ . Then we use the fact that  $c((\mathbf{X}_{1:M}, \mathbf{Y}), (\hat{\mathbf{X}}_{1:M}, \hat{\mathbf{Y}})) = \sum_{i=1}^M c_{X_i}(\mathbf{X}_i, \hat{\mathbf{X}}_i) + c_Y(\mathbf{Y}, \hat{\mathbf{Y}})$ . Finally, we follow the tower rule of expectation and the conditional independence property similar to the proof in Proposition 1 and this concludes the proof.

■

## B Encoder and Decoder Design for Multimodal Time Series Datasets

Fig. 1 illustrates how MFM operates on multimodal time series data. The encoder  $Q(\mathbf{Z}_y|\mathbf{X}_{1:M})$  can be parametrized by any model that performs multimodal fusion [10; 18; 19]. We choose the Memory Fusion Network (MFN) [18] as our encoder  $Q(\mathbf{Z}_y|\mathbf{X}_{1:M})$ . We use encoder LSTM networks and decoder LSTM networks [1] to parametrize functions  $Q(\mathbf{Z}_{a:1:M}|\mathbf{X}_{1:M})$  and  $F_{1:M}$  respectively, and FCNNs to parametrize functions  $G_y, G_{a\{1:M\}}$  and  $D$ .

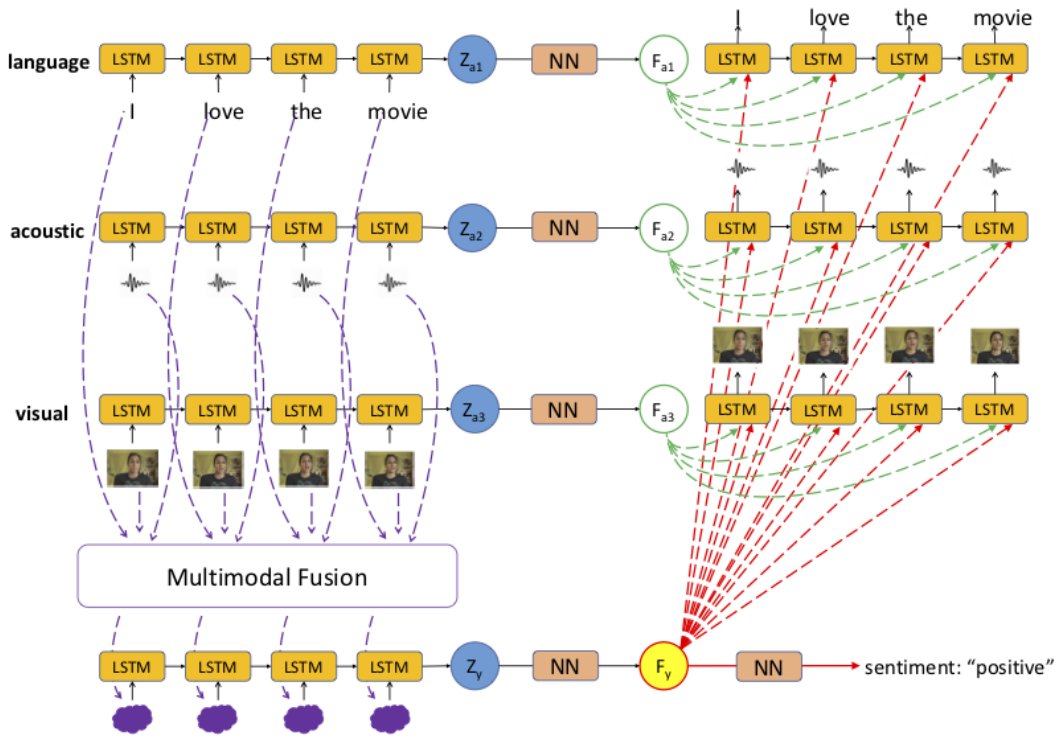


Figure 1: Recurrent neural architecture for MFM. The encoder  $Q(\mathbf{Z}_y|\mathbf{X}_{1:M})$  can be parametrized by any model that performs multimodal fusion [10; 18; 19]. We use encoder LSTM networks and decoder LSTM networks [1] to parametrize functions  $Q(\mathbf{Z}_{a_{1:M}}|\mathbf{X}_{1:M})$  and  $F_{1:M}$  respectively, and FCNNs to parametrize functions  $G_y$ ,  $G_{a_{\{1:M\}}}$  and  $D$ .

## C Multimodal Features

For each of the multimodal time series datasets as mentioned in Section 3.3, we extracted the following multimodal features: **Language:** We use pre-trained word embeddings (glove.840B.300d) [11] to convert the video transcripts into a sequence of 300 dimensional word vectors. **Visual:** We use Facet [8] to extract a set of features including per-frame basic and advanced emotions and facial action units as indicators of facial muscle movement [5; 4]. **Acoustic:** We use COVAREP [3] to extract low level acoustic features including 12 Mel-frequency cepstral coefficients (MFCCs), pitch tracking and voiced/unvoiced segmenting features, glottal source parameters, peak slope parameters and maxima dispersion quotients. To reach the same time alignment between different modalities we choose the granularity of the input to be at the level of words. The words are aligned with audio using P2FA [17] to get their exact utterance times. We use expected feature values across the entire word for visual and acoustic features since they are extracted at a higher frequencies.

## D Full Baseline Models

We use the following extra notations for full descriptions of the baseline models described in Subsection 3.3:

Variants of EF-LSTM: **EF-LSTM** (Early Fusion LSTM) uses a single LSTM [7] on concatenated multimodal inputs. We also implement the **EF-SLSTM** (stacked) [6], **EF-BLSTM** (bidirectional) [13] and **EF-SBLSTM** (stacked bidirectional) versions.



Variants of EF-HCRF: **EF-HCRF**: (Hidden Conditional Random Field) [12] uses a HCRF to learn a set of latent variables conditioned on the concatenated input at each time step. **EF-LDHCRF** (Latent Discriminative HCRFs) [9] are a class of models that learn hidden states in a CRF using a latent code between observed concatenated input and hidden output. **EF-HSSHCRF**: (Hierarchical Sequence Summarization HCRF) [15] is a layered model that uses HCRFs with latent variables to learn hidden spatio-temporal dynamics.

Variants of MV-HCRF: **MV-HCRF**: Multi-view HCRF [14] is an extension of the HCRF for Multi-view data, explicitly capturing view-shared and view specific sub-structures. **MV-LDHCRF**: [9] is a variation of the MV-HCRF model that uses LDHCRF instead of HCRF. **MV-HSSHCRF**: [15] further extends **EF-HSSHCRF** by performing Multi-view hierarchical sequence summary representation.

## E Full Results

Here we provide the full results for all baselines models described in Subsection 3.3. Table 1 contains results for multimodal speaker traits recognition on the POM dataset. Table 2 contains results for the multimodal sentiment analysis on the CMU-MOSI, ICT-MMMO and YouTube datasets. Table 3 contains results for multimodal emotion recognition on the IEMOCAP dataset. MFM consistently achieves state-of-the-art or competitive results for all five multimodal datasets. We believe that by our MFM design, the multimodal discriminative factor  $F_y$  has successfully learned more meaningful representations by distilling discriminative features. This highlights the benefit of learning factorized multimodal representations towards discriminative tasks.

Table 1: Results for personality trait recognition on the POM dataset. The best results are highlighted in bold and  $\Delta_{SOTA}$  shows the change in performance over previous state of the art. Improvements are highlighted in green. MFM achieves state-of-the-art or competitive performance on all datasets and metrics.

Dataset	POM Speaker Personality Traits															
Task	Con	Pas	Voi	Dom	Cre	Viv	Exp	Ent	Res	Tru	Rel	Out	Tho	Ner	Per	Hum
Metric	$r$															
Majority	-0.041	-0.029	-0.104	-0.031	-0.122	-0.044	-0.065	-0.105	0.006	-0.077	-0.024	-0.085	-0.130	0.097	-0.127	-0.069
SVM	0.063	0.086	-0.004	0.141	0.113	0.076	0.134	0.141	0.166	0.168	0.104	0.066	0.134	0.068	0.064	0.147
DF	0.240	0.273	0.017	0.139	0.112	0.173	0.118	0.217	0.148	0.143	0.019	0.093	0.041	0.136	0.168	0.259
EF-LSTM	0.200	0.302	0.031	0.079	0.170	0.244	0.265	0.240	0.142	0.062	0.083	0.152	0.260	0.105	0.217	0.227
EF-SLSTM	0.221	0.327	0.042	0.151	0.177	0.239	0.268	0.248	0.204	0.069	0.092	0.215	0.252	0.159	0.218	0.196
EF-BLSTM	0.162	0.289	-0.034	0.135	0.191	0.279	0.274	0.231	0.184	0.154	0.093	0.147	0.245	0.166	0.243	0.272
EF-SBLSTM	0.174	0.310	0.021	0.088	0.170	0.224	0.261	0.241	0.155	0.163	0.097	0.120	0.215	0.121	0.216	0.171
MV-LSTM	0.358	0.416	0.131	0.146	0.280	0.347	0.323	0.326	0.295	0.237	0.119	0.238	0.284	0.258	0.239	0.317
BC-LSTM	0.359	0.425	0.081	0.234	0.358	0.417	0.450	0.361	0.293	0.109	0.075	0.078	0.363	0.184	0.344	0.319
TFN	0.089	0.201	0.030	0.020	0.124	0.204	0.171	0.223	-0.051	-0.064	0.114	0.060	0.048	-0.002	0.106	0.213
MFN	0.395	0.428	0.193	0.313	0.367	0.431	0.452	0.395	0.333	0.296	0.255	0.259	0.381	0.318	0.377	0.386
MFM	<b>0.431</b>	<b>0.450</b>	<b>0.197</b>	<b>0.411</b>	<b>0.380</b>	<b>0.448</b>	<b>0.467</b>	<b>0.452</b>	<b>0.368</b>	0.212	<b>0.309</b>	<b>0.333</b>	<b>0.404</b>	<b>0.333</b>	0.334	<b>0.408</b>
$\Delta_{SOTA}$	$\uparrow 0.036$	$\uparrow 0.022$	$\uparrow 0.004$	$\uparrow 0.097$	$\uparrow 0.013$	$\uparrow 0.017$	$\uparrow 0.015$	$\uparrow 0.057$	$\uparrow 0.035$	-	$\uparrow 0.054$	$\uparrow 0.074$	$\uparrow 0.023$	$\uparrow 0.015$	-	$\uparrow 0.022$

## F Kernel Choice for Interpretation Methods

The most common choice for the kernel is the RBF kernel. However, if we consider time series data with various time steps, we need to either perform data augmentation or choose another kernel choice. For example, we can adopt the Global Alignment Kernel [2] which considers the alignment between two varying-length time series when computing the kernel score between them. To simplify our analysis, we choose to augment data before we calculate the kernel score with the RBF kernel. More specifically, we perform averaging on time series data:

$$\mathbf{X}_{aug} = \frac{1}{n} \sum_{t=1}^T X^t \text{ with } \mathbf{X} = [X^1, X^2, \dots, X^T]. \quad (5)$$

The bandwidth of the RBF kernel is set as 1.0 throughout the experiments.

Table 2: Sentiment prediction results on CMU-MOSI, ICT-MMMO and YouTube. The best results are highlighted in bold and  $\Delta_{SOTA}$  shows the change in performance over previous state of the art (SOTA). Improvements are highlighted in green. MFM achieves state-of-the-art or competitive performance on all datasets and metrics.

Dataset Task	CMU-MOSI					ICT-MMMO		YouTube	
	Sentiment					Sentiment		Sentiment	
Metric	A <sup>2</sup>	F1	A <sup>7</sup>	MAE	r	A <sup>2</sup>	F1	A <sup>3</sup>	F1
Majority	50.2	50.1	17.5	1.864	0.057	40.0	22.9	42.4	25.2
RF	56.4	56.3	21.3	-	-	70.0	69.8	33.3	32.3
SVM-MD	71.6	72.3	26.5	1.100	0.559	68.8	68.7	42.4	37.9
THMM	53.8	53.0	17.8	-	-	50.7	45.4	42.4	27.9
SAL-CNN	73.0	-	-	-	-	-	-	-	-
C-MKL	72.3	72.0	30.2	-	-	-	-	-	-
EF-HCRF	65.3	65.4	24.6	-	-	50.0	50.3	44.1	43.8
EF-LDHCRF	64.0	64.0	24.6	-	-	73.8	73.1	45.8	45.0
MV-HCRF	44.8	27.7	22.6	-	-	36.3	19.3	27.1	19.7
MV-LDHCRF	64.0	64.0	24.6	-	-	68.8	67.1	44.1	44.0
CMV-HCRF	44.8	27.7	22.3	-	-	36.3	19.3	30.5	14.3
CMV-LDHCRF	63.6	63.6	24.6	-	-	51.3	51.4	42.4	42.0
EF-HSSHCRF	63.3	63.4	24.6	-	-	50.0	51.3	37.3	35.6
MV-HSSHCRF	65.6	65.7	24.6	-	-	62.5	63.1	44.1	44.0
DF	72.3	72.1	26.8	1.143	0.518	65.0	58.7	45.8	32.0
EF-LSTM	74.3	74.3	32.4	1.023	0.622	66.3	65.0	44.1	43.6
EF-SLSTM	72.7	72.8	29.3	1.081	0.600	72.5	70.9	40.7	41.2
EF-BLSTM	72.0	72.0	28.9	1.080	0.577	63.8	49.6	42.4	38.1
EF-SBLSTM	73.3	73.2	26.8	1.037	0.619	62.5	49.0	37.3	33.2
MV-LSTM	73.9	74.0	33.2	1.019	0.601	72.5	72.3	45.8	43.3
BC-LSTM	73.9	73.9	28.7	1.079	0.581	70.0	70.1	45.0	45.1
TFN	74.6	74.5	28.7	1.040	0.587	72.5	72.6	45.0	41.0
MARN	77.1	77.0	34.7	0.968	0.625	71.3	70.2	48.3	44.9
MFN	<b>77.4</b>	<b>77.3</b>	34.1	0.965	0.632	73.8	73.1	51.7	51.6
MFM	77.3	77.2	<b>35.4</b>	<b>0.961</b>	<b>0.661</b>	<b>76.3</b>	<b>76.2</b>	<b>53.3</b>	<b>52.4</b>
$\Delta_{SOTA}$	-	-	↑ 0.7	↓ 0.004	↑ 0.029	↑ 2.5	↑ 3.1	↑ 1.6	↑ 0.8

## References

- [1] Kyunghyun Cho, Bart van Merriënboer, Çağlar Gülçehre, Dzmitry Bahdanau, Fethi Bougares, Holger Schwenk, and Yoshua Bengio. Learning phrase representations using rnn encoder-decoder for statistical machine translation. In *Proceedings of the 2014 Conference on Empirical Methods in Natural Language Processing (EMNLP)*, pages 1724–1734, Doha, Qatar, October 2014. Association for Computational Linguistics.
- [2] Marco Cuturi, Jean-Philippe Vert, Oystein Birkenes, and Tomoko Matsui. A kernel for time series based on global alignments. In *Acoustics, Speech and Signal Processing, 2007. ICASSP 2007. IEEE International Conference on*, volume 2, pages II–413. IEEE, 2007.
- [3] Gilles Degottex, John Kane, Thomas Drugman, Tuomo Raitio, and Stefan Scherer. Covarepa collaborative voice analysis repository for speech technologies. In *Acoustics, Speech and Signal Processing (ICASSP), 2014 IEEE International Conference on*, pages 960–964. IEEE, 2014.
- [4] Paul Ekman. An argument for basic emotions. *Cognition & emotion*, 6(3-4):169–200, 1992.
- [5] Paul Ekman, Wallace V Freisen, and Sonia Ancoli. Facial signs of emotional experience. *Journal of personality and social psychology*, 39(6):1125, 1980.
- [6] A. Graves, A. r. Mohamed, and G. Hinton. Speech recognition with deep recurrent neural networks. In *2013 IEEE International Conference on Acoustics, Speech and Signal Processing*, pages 6645–6649, May 2013.
- [7] Sepp Hochreiter and Jürgen Schmidhuber. Long short-term memory. *Neural computation*, 9(8):1735–1780, 1997.
- [8] iMotions. Facial expression analysis, 2017.

Table 3: Emotion recognition results on IEMOCAP test set. The best results are highlighted in bold and  $\Delta_{SOTA}$  shows the change in performance over previous SOTA. Improvements are highlighted in green. MFM achieves state-of-the-art or competitive performance on all datasets and metrics.

Dataset Task Metric	IEMOCAP Emotions											
	Happy		Sad		Angry		Frustrated		Excited		Neutral	
	A <sup>2</sup>	F1	A <sup>2</sup>	F1	A <sup>2</sup>	F1	A <sup>2</sup>	F1	A <sup>2</sup>	F1	A <sup>2</sup>	F1
Majority	85.6	79.0	79.4	70.3	75.8	65.4	79.5	70.4	89.6	84.7	59.1	44.0
SVM	86.1	81.5	81.1	78.8	82.5	82.4	77.3	71.1	86.4	86.0	65.2	64.9
RF	85.5	80.7	80.1	76.5	81.9	82.0	78.6	75.3	88.9	85.1	63.2	57.3
THMM	85.6	79.2	79.5	79.8	79.3	73.0	71.6	69.6	86.0	84.6	58.6	46.4
EF-HCRF	85.7	79.2	79.4	70.3	75.8	65.4	79.5	70.4	89.6	84.7	59.1	44.0
EF-LDHCRF	85.8	79.5	79.4	70.3	75.8	65.4	79.5	70.4	89.6	84.7	59.1	44.0
MV-HCRF	15.0	4.9	79.4	70.3	24.2	9.4	79.5	70.4	89.6	84.7	59.1	44.0
MV-LDHCRF	85.7	79.2	79.4	70.3	75.8	65.4	79.5	70.4	89.6	84.7	59.1	44.0
CMV-HCRF	14.4	3.6	79.4	70.3	24.2	9.4	79.5	70.4	89.6	84.7	59.1	44.0
CMV-LDHCRF	85.8	79.5	79.4	70.3	75.8	65.4	79.5	70.4	89.6	84.7	59.1	44.0
EF-HSSHCRF	85.8	79.5	79.4	70.3	75.8	65.4	79.5	70.4	89.6	84.7	59.1	44.0
MV-HSSHCRF	85.8	79.5	79.4	70.3	75.8	65.4	79.5	70.4	89.6	84.7	59.1	44.0
DF	86.0	81.0	81.8	81.2	75.8	65.4	78.4	76.8	89.6	84.7	59.1	44.0
EF-LSTM	85.2	83.3	82.1	81.1	84.5	84.3	79.5	70.4	89.6	84.7	68.2	67.1
EF-SLSTM	85.6	79.0	80.7	80.2	82.8	82.2	77.5	69.7	89.3	86.2	68.8	<b>68.5</b>
EF-BLSTM	85.0	83.7	81.8	81.6	84.2	83.3	79.5	70.4	89.6	84.7	67.1	66.6
EF-SBLSTM	86.0	84.2	80.2	80.5	85.2	84.5	79.5	70.4	89.6	84.7	67.8	67.1
MV-LSTM	85.9	81.3	80.4	74.0	85.1	84.3	79.5	73.8	88.9	85.8	67.0	66.7
BC-LSTM	84.9	81.7	83.2	81.7	83.5	84.2	80.0	76.1	86.9	85.4	67.5	64.1
TFN	84.8	83.6	83.4	82.8	83.4	84.2	74.1	74.3	75.6	78.0	67.5	65.4
MARN	86.7	83.6	82.0	81.2	84.6	84.2	79.5	76.6	89.6	<b>87.1</b>	66.8	65.9
MFN	90.1	85.3	85.8	79.2	87.0	86.0	80.3	<b>76.9</b>	89.8	86.3	71.8	61.7
MFM	<b>90.2</b>	<b>85.8</b>	<b>88.4</b>	<b>86.1</b>	<b>87.5</b>	<b>86.7</b>	<b>80.4</b>	74.5	<b>90.0</b>	<b>87.1</b>	<b>72.1</b>	68.1
$\Delta_{SOTA}$	↑0.1	↑0.5	↑2.6	↑3.3	↑0.5	↑0.7	↑0.1	–	↑0.2	–	↑0.3	–

- [9] Louis-Philippe Morency, Ariadna Quattoni, and Trevor Darrell. Latent-dynamic discriminative models for continuous gesture recognition. In *Computer Vision and Pattern Recognition, 2007. CVPR'07. IEEE Conference on*, pages 1–8. IEEE, 2007.
- [10] Behnaz Nojavanasghari, Deepak Gopinath, Jayanth Koushik, Tadas Baltrušaitis, and Louis-Philippe Morency. Deep multimodal fusion for persuasiveness prediction. In *Proceedings of the 18th ACM International Conference on Multimodal Interaction, ICMI 2016*, pages 284–288, New York, NY, USA, 2016. ACM.
- [11] Jeffrey Pennington, Richard Socher, and Christopher D Manning. Glove: Global vectors for word representation. In *EMNLP*, volume 14, pages 1532–1543, 2014.
- [12] Ariadna Quattoni, Sybor Wang, Louis-Philippe Morency, Michael Collins, and Trevor Darrell. Hidden conditional random fields. *IEEE Trans. Pattern Anal. Mach. Intell.*, 29(10):1848–1852, October 2007.
- [13] M. Schuster and K.K. Paliwal. Bidirectional recurrent neural networks. *Trans. Sig. Proc.*, 45(11):2673–2681, November 1997.
- [14] Yale Song, Louis-Philippe Morency, and Randall Davis. Multi-view latent variable discriminative models for action recognition. In *Computer Vision and Pattern Recognition (CVPR), 2012 IEEE Conference on*, pages 2120–2127. IEEE, 2012.
- [15] Yale Song, Louis-Philippe Morency, and Randall Davis. Action recognition by hierarchical sequence summarization. In *Proceedings of the IEEE Conference on Computer Vision and Pattern Recognition*, pages 3562–3569, 2013.
- [16] Ilya Tolstikhin, Olivier Bousquet, Sylvain Gelly, and Bernhard Schoelkopf. Wasserstein auto-encoders. *arXiv preprint arXiv:1711.01558*, 2017.

- [17] Jiahong Yuan and Mark Liberman. Speaker identification on the scotus corpus. *Journal of the Acoustical Society of America*, 123(5):3878, 2008.
- [18] Amir Zadeh, Paul Pu Liang, Navonil Mazumder, Soujanya Poria, Erik Cambria, and Louis-Philippe Morency. Memory fusion network for multi-view sequential learning. *Proceedings of the Thirty-Second AAAI Conference on Artificial Intelligence*, 2018.
- [19] Amir Zadeh, Paul Pu Liang, Soujanya Poria, Prateek Vij, Erik Cambria, and Louis-Philippe Morency. Multi-attention recurrent network for human communication comprehension. *Proceedings of the Thirty-Second AAAI Conference on Artificial Intelligence*, 2018.